Journal of Biomolecular NMR, 3 (1993) 55–66
ESCOM

J-Bio NMR 101

Structure refinement using time-averaged J-coupling constant restraints

Andrew E. Torda[a,*], Roger M. Brunne[a], Thomas Huber[b], Horst Kessler[b] and Wilfred F. van Gunsteren[a]

[a]*Physical Chemistry (Computational Chemistry), ETH Zentrum, CH-8092 Zürich, Switzerland*
[b]*Organisch-Chemisches Institut, Technische Universität München, D-8046 Garching, Germany*

Received 6 July 1992
Accepted 22 October 1992

Keywords: J-coupling; Time averaging; Structure refinement; Computer simulation; Molecular dynamics

SUMMARY

We describe a new penalty function for use in restrained molecular dynamics simulations which allows experimental J-coupling information to be enforced as a time-averaged, rather than instantaneous, quantity. The pseudo-energy term has been formulated in terms of a calculated J value (a measured quantity) rather than the relevant dihedral angle (a derived quantity). This accounts for the distinct non-linearity of the coupling constant with respect to either Cartesian coordinates or dihedral angles. Example simulations of the cyclic decapeptide antamanide show the procedure's ability to enforce experimental restraints while exploring a large region of conformational space and producing a relatively small disturbance of the physical force field.

INTRODUCTION

When calculating solution structures from NMR data, the bulk of experimental data are nuclear Overhauser effect (NOE) distance restraints. Vicinal ^3J coupling constants should complement this information since one can directly relate them back to a geometrical parameter, the included dihedral angle, θ, through the Karplus equation:

$$J(\theta) = a \cos^2(\theta) + b \cos(\theta) + c, \quad (1)$$

where $J(\theta)$ is the measured coupling constant, and a, b and c are constants of calibration (Karplus, 1959).

* To whom correspondence should be addressed.
Abbreviations: MD, molecular dynamics; rms, root-mean-square; NOE, nuclear Overhauser effect.

Val	Pro	Pro	Ala	Phe	Phe	Pro	Pro	Phe	Phe
1	2	3	4	5	6	7	8	9	10

Fig. 1. Sequence of the cyclic peptide antamanide.

Unfortunately, there are several restrictions on the use of this information. Firstly, the measured coupling constant is not the result of a single conformation. It is a weighted average of J values for all solution conformations accessible to the molecule at the temperature of the measurement and averaged on the NMR time scale. This, in turn, is a distinctly non-linear average with respect to either Cartesian coordinates or dihedral angles. The geometric solution of Eq. 1 may not even represent a physically plausible conformation for some sets of coupling constants (Jardetzky, 1980).

A proper treatment of coupling constant information should therefore include a time axis, as in a MD trajectory, and account for the non-linear relationship between spectroscopic and geometric parameters.

The problem of enforcing a restraint as a time average has been treated for the case of distance restraints (Torda et al., 1989, 1990; Pearlman and Kollman, 1991). Here, we apply a similar approach to J-coupling restraints. A second problem of non-linear parameter dependence can be treated by formulating a penalty function or pseudo-energy term as a function of the spectroscopic parameter, the measured ^3J vicinal coupling constant (Kim and Prestegard, 1990; Mierke and Kessler, 1992).

To assess this method of enforcing coupling constant information, we conducted a series of simulations for the cyclic peptide antamanide whose sequence is shown in Fig. 1. This was an interesting test system as previous studies found no single conformation which could explain the experimental homonuclear coupling constants (Kessler et al., 1988, 1989; Brüschweiler et al., 1991). Kessler et al. (1988) proposed that a combination of between two and four structures would be necessary to explain the experimental data. In contrast, a time-averaged restraint approach should be able to treat the data in a more automatic and less ad hoc manner.

THEORY

In order to enforce some experimental restraint on a simulated system, a potential energy term is constructed such that its value will rise as the restraint is violated. In the case of a coupling constant restraint, several possibilities exist for defining V_J the pseudo-energy associated with J-coupling restraint data. First, one could calculate a corresponding dihedral angle, θ, from Eq. 1 and define a quadratic potential with respect to the difference between θ and a reference angle, θ_0 (Clore et al., 1986),

$$V_J = \frac{K_J}{2}(\theta - \theta_0)^2 \qquad (2)$$

The decision to make the energy increase quadratically with respect to dihedral angles is, how-

ever, arbitrary and has no physical basis. Alternatively, one could define V_J in a similar manner to the dihedral angle term in the physical force field:

$$V_J = K_J(1 + \cos(\theta - \theta_0)), \tag{3}$$

where θ_0 is chosen so the potential goes to zero when the system is at the desired angle (de Vlieg et al., 1986). This formulation also has no real basis when considered in terms of errors with respect to the measured J-couplings.

A more natural potential energy term can be constructed as described by Kim and Prestegard (1990):

$$V_J = \frac{K_J}{2}(J(\theta) - J_0)^2, \tag{4}$$

where J_0 is the measured coupling constant. This may be considered an improvement over Eqs 2 and 3 since the potential energy is quadratic with respect to the error in the spectroscopic parameter rather than some arbitrary geometric parameter.

In order to incorporate time-averaged restraints, one must remember that the angle is a time-dependent function and properly referred to as $\theta(t)$. A potential energy term can now be defined in terms of the time-averaged J value, which we denote $\bar{J}(\theta(t))$

$$V_J = \frac{K_J}{2}(\bar{J}(\theta(t)) - J_0)^2. \tag{5}$$

$\bar{J}(\theta(t))$ must then be defined. One could sum over the course of a MD simulation:

$$\bar{J}(\theta(t)) = \frac{1}{t}\int_0^t J(\theta(t'))dt'. \tag{6}$$

Equation 6 is the true average coupling constant and is used in the analysis of MD trajectories, but it is not suitable for deriving a force during the finite time of a MD simulation. As time increases, and $\bar{J}(\theta(t))$ is calculated over a longer period, the average becomes less sensitive to instantaneous fluctuations. As with time-averaged distance restraints, this problem can be avoided by building a decay into the summation over time with a characteristic decay time, τ, so that

$$\bar{J}(\theta(t)) = [\tau(1-\exp(-t/\tau))]^{-1}\int_0^t \exp(-t'/\tau)J(\theta(t-t'))dt'. \tag{7}$$

In practice, we do not implement Eq. 7 directly. For convenience, we use a formulation in terms of the cosine of the angle. The average coupling constant can be written in terms of the Karplus equation expressed in terms of the time-averaged cosine,

$$\bar{J}(\theta(t)) = a\,\overline{\cos^2\theta(t)} + b\,\overline{\cos\theta(t)} + c, \tag{8}$$

and for an arbitrary power, m, one can write

$$\overline{\cos^m\theta(t)} = \frac{1}{\tau(1 - e^{\frac{-t}{\tau}})} \int_0^t e^{(-\frac{t-t'}{\tau})} \cos^m\theta(t')dt'. \quad (9)$$

We can then simplify Eq. 9 and write it in a discrete form suitable for a MD simulation. First, one notes that if $t \gg \tau$, then

$$1 - e^{\frac{-t}{\tau}} \approx 1, \quad (10)$$

and Eq. 9 becomes

$$\overline{\cos^m\theta(t)} \approx (1 - e^{\frac{-\Delta t}{\tau}}) \cos^m\theta(t) + e^{\frac{-\Delta t}{\tau}}\overline{\cos^m\theta(t-\Delta t)}, \quad (11)$$

where Δt is the time step of the integrator in the simulation.

In the simulations described below, Eq. 11 was calculated and substituted into Eq. 8, and the potential energy was calculated from Eq. 5. One should also note that a derivative with respect to coordinates calculated from Eq. 11 includes a term which is scaled by $(1-e^{-\Delta t/\tau})$, so the force constant K_J is scaled appropriately.

METHODS

Newtonian MD simulations of small systems in vacuo can display artefactual inertial motions and highly correlated motions. To avoid this problem, all simulations were performed using a stochastic dynamics algorithm (Shi Yun-yu et al., 1988; van Gunsteren and Berendsen, 1988). At each time step, one solves the Langevin equation:

$$m_i\frac{dv_i(t)}{dt} = F_i(x_i(t)) - m_i\gamma_i v_i(t) + R_i(t) \quad (12)$$

where m_i, v_i, F_i and x_i have their conventional meanings of mass, velocity, force and coordinate of particle i, respectively. R_i is an uncorrelated force mimicking the stochastic influence of the solvent and γ_i is a friction coefficient for the atom. In accordance with as yet unpublished results, we set

$$\gamma_i = \omega_i\gamma \quad (13)$$

where $\gamma = 19$ ps^{-1} and ω_i is a weighting factor given to each atom according to a crude estimate of the atom's solvent accessibility. ω_i is set to 1 if an atom has no neighbouring solute atoms within a radius of 3 Å and is decreased stepwise to zero as the number of neigbouring atoms rises to 6 or more.

All simulations were carried out using software from the GROMOS suite of programs with the GROMOS force field (van Gunsteren and Berendsen, 1987). A time step of 0.002 ps was used in the integrator and the system was weakly coupled ($\tau = 0.1$ ps) to a heating bath at 300 K

(Berendsen et al., 1984). The SHAKE algorithm was used to constrain bond lengths (Ryckaert et al., 1977) and no cut-offs were used for long-range interactions.

J-coupling restraints were imposed according to Eq. 5, with a force constant of $K_J = 16(1 - e^{-\Delta t/\tau})^{-1}$ kJ mol^{-1} s^2. In calculations with time-averaged restraints, the decay constant for the memory function was τ=50 ps and the initial value for $\bar{J}(\theta(t))$ was set to the calculated ^3J value at the first time step.

The starting structure for all simulations was the best single structure taken from Brüschweiler et al. (1991), judged by agreement with experimental data. Using the dihedral angle classification of Kessler et al. (1988), this structure corresponds to the X-ray structure of Karle et al. (1979). The energy was minimized to relax the system in the GROMOS force field and the molecule was then subjected to a 10-ps stochastic dynamics equilibration run.

Experimental restraints consisted of the six homonuclear coupling constants given in Table 2 of Kessler et al. (1988) and shown in Table 1 of the Results section. Equation 1 was calculated using the calibration constants from Bystrov (1976), where a = 9.4, b = −1.1 and c = 0.4. Although more recent calibrations exist (Pardi et al., 1984; Ludvigsen et al., 1991), the older values were used to allow comparison with the work of Kessler et al. (1988). No distance restraints were imposed.

RESULTS

The simplest test of time-averaged coupling constant restraints is a comparison of simulations with restraints enforced according to Eq. 5 (time-averaged) or with τ=0, which reduces to Eq. 4 (conventional, instantaneous restraints). Table 1 compares the experimental ^3J values with trajectory averages for two such 1-ns simulations. The quoted coupling constants were averaged over whole trajectories, calculated according to Eq. 6.

From Table 1, it appears that both schemes for coupling constant restraints were capable of producing a trajectory which explains the experiment to within 0.3 Hz. The difference in the simulations is, however, clear from the rms fluctuations. With conventional, instantaneous restraints, the fluctuations were uniformly 0.4 Hz. This reflects system motion being restricted by the artificial potential energy wells created by the pseudo-energy term. The exact size of the fluctuations was effectively controlled by K_J and, in this simple test case, one can see how the pseudo-energy terms effectively determined the dynamics of the system. With time-averaged restraints, the fluctuations were typically 5- to 7-fold larger. The range of these motions reflects several influences. First, the natural motions of the system will dominate if the restraints are, on average, satisfied. Second, the system is, at times, driven from one conformation to another, so the fluctuations represent the motions necessary to explain the experimental data.

Not surprisingly, the conventionally restrained trajectory average ^3J had a relatively large error for coupling constants corresponding to the φ angles of Phe^5 and Phe^{10}. In the earlier work of Kessler et al. (1988), it was postulated that the NMR results represented an average of two conformations at each of these two locations. Consequently, a method which models NMR structures as single conformations will never be able to reproduce the data properly. In contrast, the time-averaged run was able to reproduce both coupling constants to within 0.1 Hz.

Noting that we imposed few experimental restraints on the system, and that the run with large fluctuations was able to satisfy the NMR data, it was of interest to see if large additional mobility

TABLE 1
$^3J_{HCN\alpha H}$ COUPLING CONSTANTS AND POTENTIAL ENERGIES IN ANTAMANIDE SIMULATIONS[a]

	^{3}J(Hz)			
	Experimental	Simulation		
		Restrained		Unrestrained
		Time-averaged	Conventional	
Val[1]	7.3	7.5 ± 3.0	7.4 ± 0.4	10.1 ± 1.8
Ala[4]	8.6	8.6 ± 1.9	8.6 ± 0.4	6.9 ± 2.2
Phe[5]	6.8	6.7 ± 2.1	7.0 ± 0.4	7.9 ± 2.0
Phe[6]	6.6	6.9 ± 2.9	6.7 ± 0.4	10.1 ± 1.0
Phe[9]	8.3	8.2 ± 2.1	8.3 ± 0.4	6.8 ± 2.8
Phe[10]	6.7	6.6 ± 2.0	7.0 ± 0.4	8.0 ± 1.9
averaged over		1 ns	1 ns	0.5 ns
E_{pot} (kJ mol^{-1})		328 ± 24	380 ± 20	329 ± 32

[a] Experimental values were taken from Kessler et al. (1988). Calculated ^{3}J values are full trajectory averages calculated according to Eq. 6 over the indicated length of time. Both coupling constants and potential energies are shown with rms fluctuations.

alone is enough to ensure agreement with experimental data. Table 1 shows the results from a shorter (500 ps) unrestrained simulation. Although the fluctuations were of similar size to the run with time-averaged restraints, the average ^{3}J values showed the worst agreement with the experimental data. Clearly it is not sufficient for the molecule to drift through conformational space under the influence of only the physical force field. Restraints are necessary if one wants a trajectory that explains the experimental data.

As an additional check on the physical plausibility of the time-averaged structures, Table 1 also shows the mean potential energy of the system, without pseudo-energy terms, averaged over the trajectories. The differences between the runs were not great in the context of the rms fluctuations, but do reflect the different conditions in the different simulations. The run with conventional restraints must have a higher energy than the unrestrained trajectory. By simply adding a potential term that is always zero or positive, one ensures that the system will traverse a higher-energy path. In the case of J-coupling restraints representing a mix of different conformers, the situation is somewhat worse. The conventional restraints may well push the molecule towards some mean structure which does not correspond to a minimum in the physical force field. The situation with time-averaged restraints is again different. If restraints are satisfied most of the time, the system will travel towards physical minima because it is not penalized for instantaneous violations. If, however, a violation builds up over time, the potential energy surface is shifted with respect to coordinates and the system is driven to satisfy the experimental data and possibly move into a different minimum in the physical force field. Although this driving behaviour requires energy, which was supplied by the heating bath, and the force-field is no longer strictly conservative, Table 1 shows that the mean potential energy was undisturbed. Apparently, the system was

mainly in physical minima rather than unrealistic transition states. This is exactly the behaviour that one requires if a trajectory is to sample conformational space realistically within the restrictions of the experimental data.

DISCUSSION

As with distance restraints, the introduction of time averaging greatly increases the conformational space spanned by a trajectory during a refinement calculation. With a simple system like antamanide, it is possible to examine some of the physical aspects in more detail. For example, one can look at the behaviour of the restrained dihedral angle, φ, of Phe[10]. In the earlier work of Kessler et al. (1988), it appeared that the experimental results could only be explained by the existence of two conformers with angles of about 58° and −83°. Referring to Fig. 2, one can see that both of these angles will result in ^3J values near 6.7 Hz, the target value from experiment. Figure 3 shows the φ angle from Phe[10] over the course of the trajectories with time-averaged and conventional restraints. With instantaneous restraints, the system fell into a minimum resulting from the sum of physical and pseudo-energy terms and was unable to move to satisfy the experimental restraint. This led to the residual ^3J violation of 0.3 Hz seen in Table 1. Apparently there is some structural hindrance to rotation about the dihedral angle, so the system never moved to exactly the desired ^3J. In contrast, the run with time-averaged restraints showed great mobility, but, on average, was able to satisfy the restraint within 0.1 Hz (Table 1). Surprisingly, the φ angle remained near −80° for the whole simulation and the increased fluctuations alone were able to account for the experimental coupling constant without having to invoke a substantially different conformation. It must be remembered that this does not contradict the earlier interpretation of Kessler et al. (1988). Our aim was to test a form for J-coupling restraints, so the

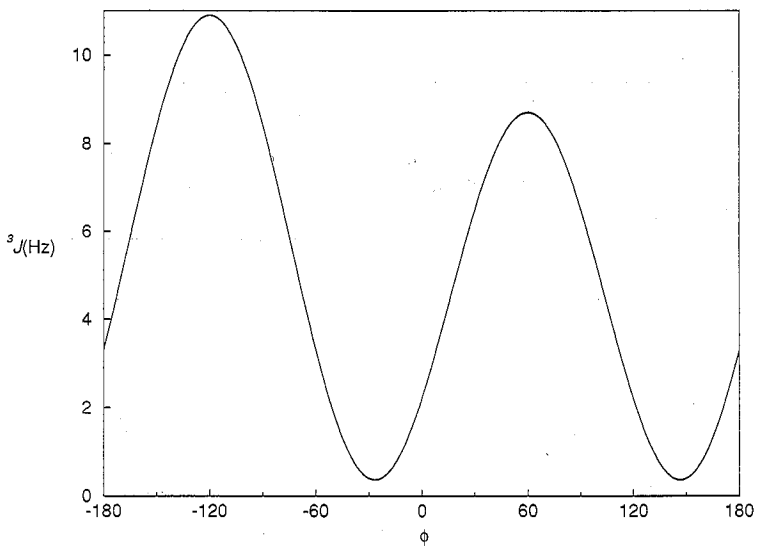

Fig. 2. The Karplus curve, Eq. 1, with the calibration constants of Bystrov (1976), a = 9.4, b = −1.1, c = 0.4. A 60°-phase shift was used so the angle φ is expressed in conventional protein nomenclature.

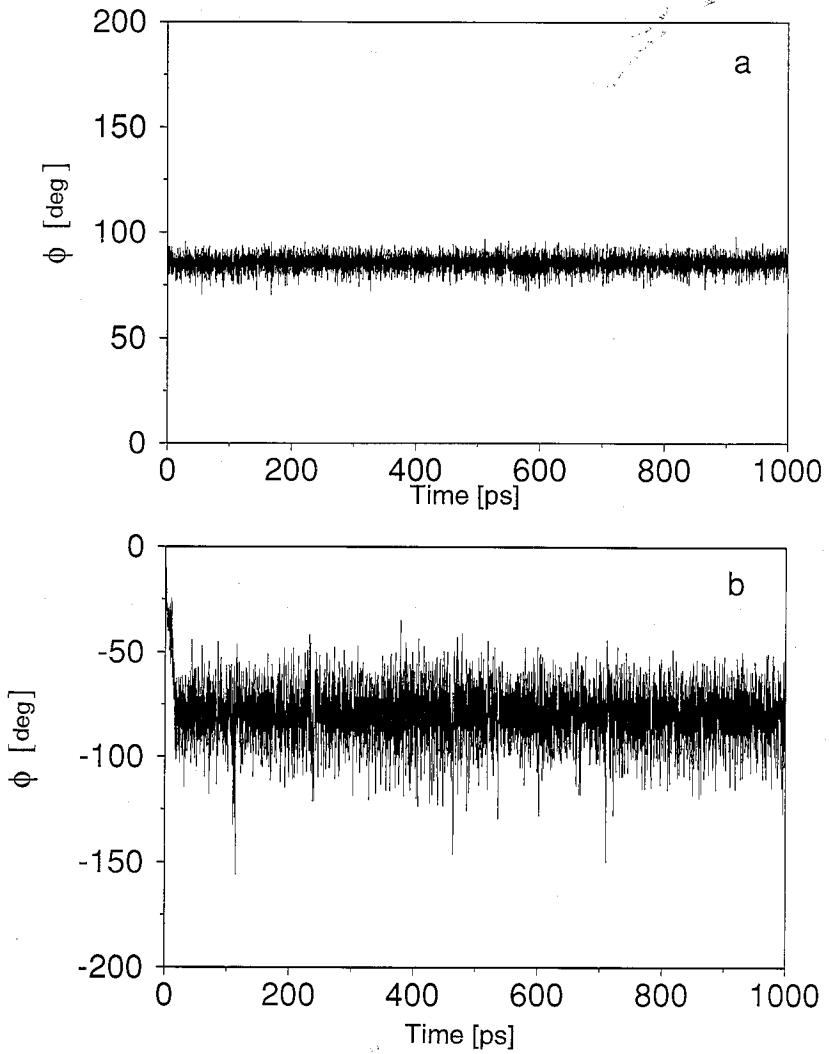

Fig. 3. φ Angle of Phe[10] over the course of 1-ns simulations with (a) instantaneous restraints according to Eq. 4, and (b) time-averaged restraints according to Eq. 5.

simulations did not include the NOE distance restraints. Including these may have forced the system to move between different conformers. All this result shows is that this trajectory displays the minimum of motion necessary to comply with the NMR measurements.

A different behaviour is shown by the φ angle of Phe[6]. This was not amongst the sites identified by Kessler et al. (1988) as displaying conformational averaging. Figure 4a shows how the instantaneous ^3J was able to drive the system to a single minimum which reproduced the experimental data. At the same time, the corresponding plot from the time-averaged run (Fig. 4b) shows that the system hopped between two distinct conformations ($\varphi \approx -70°$ and $\varphi \approx -160°$), both of which were close to agreeing with the observed coupling constant. Not having used the NOE data, it is not possible to state that this is the actual behaviour in solution. It does, however, show an

important limitation of instantaneous restraints when modelling a dynamic system. In a conventionally restrained simulation, the system may be driven away from minima in the physical force field to satisfy the experimental data. With time-averaged restraints, the system will attempt to move between the closest physical minima in order to agree with the experiment. This should ensure a trajectory which more closely follows physical reality.

Figure 4 also shows another property of time-averaged restraints. For the first 40–50 ps, there was relatively little motion about the torsion angle, whereafter the system moved to the pattern of hopping between two conformations. At the start of the simulation, the average, $\bar{J}(\theta(t))$, was not defined, so we set it to the instantaneous $J(\theta(t))$ at the first time step. This means that, at the start of the calculation, $(\bar{J}(\theta(t))-\bar{J}_0)^2$ may have been non-zero for several restraints and the system was initially rigid, as it would be with conventional restraints. Further into the trajectory, the natural motions of the system were apparently enough to satisfy some restraints and remove barriers to motion. In a small molecule like antamanide in vacuo, this is not a problem as long simulation times are not computationally expensive. In a larger system, it might be advisable to set an initial value for $\bar{J}(\theta(t))$ so that no restraints are violated at the first step. This was the approach we used previously with a large polypeptide and time-averaged distance restraints (Torda et al., 1990).

The use of time-averaged restraints has further implications for the type of data that can be used in a refinement calculation. At present, there is no consensus as to what constitutes a useful restraint. Braun (1987) points out that, due to molecular flexibility, one should only use extreme values from the Karplus curve where averaging will only have a small effect (see Fig. 2). Unfortunately, what constitutes extreme is an arbitrary decision. For example, this could be ^3J values greater than 9 Hz (Clore et al., 1987) or 8 Hz (Wagner et al., 1987; Driscoll et al., 1989). With time-averaged restraints, this problem is alleviated somewhat. This can be seen by looking at the fluctuation of $^3J_{HNC\alpha H}$ from Phe^6. The experimental value of the coupling constant was 6.6 Hz and would not normally be used in a refinement calculation. Figure 5 shows the $^3J_{HNC\alpha H}$ calculated over the trajectory. Remarkably, the instantaneous $^3J_{HNC\alpha H}$ values, marked by the dots, spanned the entire range allowed by the Karplus curve. This is understandable when one considers Fig. 4, which shows the corresponding φ angle. Whilst undergoing the transitions necessary to reproduce the experimental data, the system must temporarily move through regions of space which would be effectively forbidden with instantaneous restraints. Figure 5 also highlights some other properties of time-averaged restraints. The solid line marks in the $\bar{J}(\theta(t))$ values calculated from Eq. 7 and thus the value used to calculate the force during the simulation. Although the instantaneous coupling constant takes on extreme values, $\bar{J}(\theta(t))$ never moved far away from the target value of 6.6 Hz, so no large artificial forces were put into the simulation. This is another reason why one can expect more realistic trajectories with time-averaged rather than conventional, instantaneous restraints. Figure 5 also suggests that for this small system, the choice of τ = 50 ps was long enough to allow relatively unhindered motions. Although the major conformational changes for this dihedral angle occurred every few hundred picoseconds (Fig. 4), the motions which provided the averaging occurred much faster than τ, so the choice of decay constant had little effect on these fluctuations. Of course, in the case of averaging over slower motions, the choice of τ may well be such as to drive the system across barriers and distort the time scale of the dynamics. The dashed line shows the value of $\bar{J}(\theta(t))$ calculated according to Eq. 6 and is thus the average without a memory function up to each point in the trajectory. It is this value (the entire trajectory

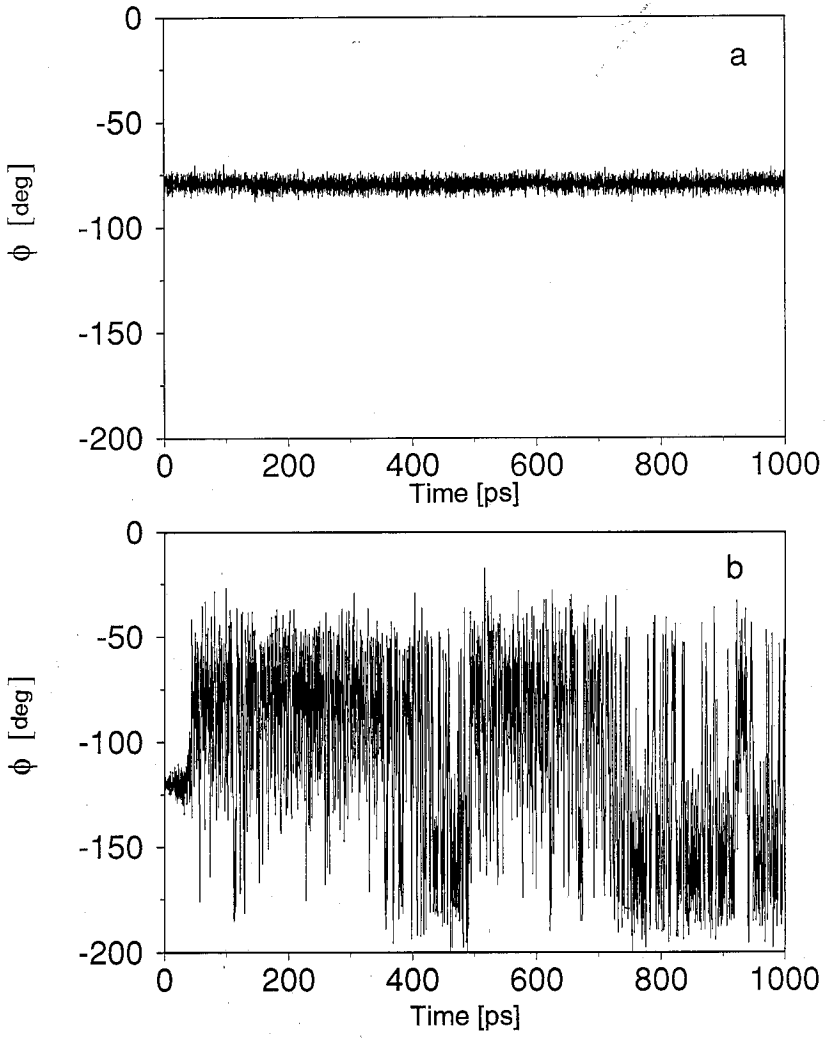

Fig. 4. φ Angle of Phe[6] over the course of 1-ns simulations with (a) instantaneous restraints according to Eq. 4, and (b) time-averaged restraints according to Eq. 5.

average) which must satisfy the restraints. The curve shows slow convergence and suggests that, as with distance restraints, the use of time averaging necessitates longer simulations.

It is of interest to contrast our approach with that of Kim and Prestegard (1990) in two respects. First, Kim and Prestegard used Eq. 4 to enforce coupling constant restraints through the instantaneous calculated ^3J. As they pointed out, certain values of ^3J correspond to more than one dihedral angle (see Fig. 2). Ideally, steric restrictions and additional NOE restraints will drive the system to the correct dihedral angle. Unfortunately, the system may fall into the false minimum created by such a pseudo-energy term and become trapped in the wrong conformation. The form of Eq. 4 is such that a wrong solution is just as favourable as the correct one. While our formulation will not select the correct dihedral angle, at least it will allow the system to move

away from wrong solutions. Second, Kim and Prestegard addressed the problem of multiple conformations by starting parallel simulations from two different conformations and defining

$$J(\theta) = f_1 J_1(\theta) + f_2 J_2(\theta), \tag{14}$$

where f_1 and f_2 are the fractional populations of two different conformations. This approach models the conformational space of a molecule as a very small number of well defined states. Furthermore, these states must be identified before one can perform the simulation and one must use some approximation to estimate f_1 and f_2 since they depend on the free energy difference, which is not a known quantity during a simulation. In contrast, our approach models the conformational space of a molecule as a continuum and makes no assumptions in advance about distinct conformational states. The advantage of not making prior assumptions can be seen in the calculations where we were able to explain the $^3J_{HNC\alpha H}$ coupling constant of Phe[10] without invoking the two conformations of Kessler et al. (1988). Our approach also has the advantage that it scales to arbitrarily complex systems. In our previous work with time-averaged distance restraints, one could see conformational averaging in a large polypeptide where no evidence of multiple conformations had been previously proposed and where the system size would make it impractical to attempt to identify all the possible substates. Lastly, one should note that with our approach the problem of having to assign weights to individual conformers, as would be necessitated by Eq. 14, is avoided. With our approach, the system distributes itself over the potential surface (including the penalty function) with a Boltzmann distribution and entropic effects are automatically included.

We should also note a substantial advantage that the Kim and Prestegard (1990) formulation has. It may well happen that a measurement reflects conformations which are in fast exchange on the NMR time scale, but which are totally inaccessible on the much shorter simulation time scale. If the energetic barriers are much greater than k_BT, the transitions will not occur during a simulation and one will require an approach similar to Eq. 14 to reproduce the experimental data.

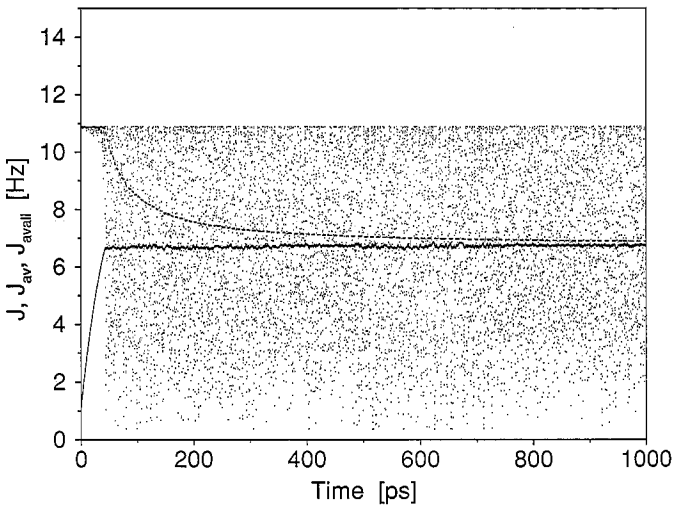

Fig. 5. $^3J_{HNC\alpha H}$ calculated for Phe[6] over the 1-ns simulation using time-averaged coupling constant restraints. The solid line shows the value calculated with the memory function according to Eq. 7 and used to calculate the force. The dashed line shows $\bar{J}(\theta(t))$ calculated according to Eq. 6. The dots mark instantaneous values for $^3J_{HNC\alpha H}$.

CONCLUSIONS

If one is interested in a non-physical and possibly energetically stressed mean conformation, then restraints based on instantaneous values will be adequate. If, however, one intends to use a structure for a purpose such as molecular modelling, then it would not be wise to ignore the range of conformations adopted by a molecule in solution. The use of time-averaged restraints allows one to estimate better the conformational space that is consistent with the experimental data. It also permits trajectories which are less perturbed by pseudo-energy terms and which model solution behaviour more closely. In the case of coupling constant restraints, it also allows one to use more experimental data than was previously possible.

With a combination of time-averaged distance restraints and coupling constant restraints it might be interesting to re-assess some structures reported in the literature and to see exactly what additional information can be extracted from existing experimental data.

REFERENCES

Berendsen, H.J.C., Postma, J.P.M., van Gunsteren, W.F., DiNola, A. and Haak, J.R. (1984) *J. Chem. Phys.*, **81,** 3684–3690.

Braun, W. (1987) *Q. Rev. Biophys.*, **19,** 115–157.

Brüschweiler, R., Blackledge, M. and Ernst, R.R. (1991) *J. Biomol. NMR,* **1,** 3–11.

Bystrov, V.F. (1976) *Progr. NMR Spectrosc.*, **10,** 41–81.

Clore, G.M., Nilges, M., Sukumaran, D.K., Brünger, A.T., Karplus, M. and Gronenborn, A.M. (1986) *EMBO J.*, **5,** 2729–2735.

Clore, G.M., Sukumaran, D.K., Nilges, M. and Gronenborn, A.M. (1987) *Biochemistry,* **26,** 1732–1745.

De Vlieg, J., Boelens, R., Scheek, R.M., Kaptein, R. and van Gunsteren, W.F. (1986) *Isr. J. Chem.*, **27,** 181–188.

Driscoll, P.C., Gronenborn, A.M., Beress, L. and Clore, G.M. (1989) *Biochemistry,* **28,** 2188–2198.

Jardetzky, O. (1980) *Biochim. Biophys. Acta.*, **621,** 227–232.

Karle, I.L., Wieland, T., Schermer, D. and Ottenheym, H.C.J. (1979) *Proc. Natl. Acad. Sci. USA,* **76,** 1532–1536.

Karplus, M. (1959) *J. Chem. Phys.*, **30,** 11–15.

Kessler, H., Griesinger, C., Lautz, J., Müller, A., van Gunsteren, W.F. and Berendsen, H.J.C. (1988) *J. Am. Chem. Soc.*, **110,** 3393–3396.

Kessler, H., Bats, J.W., Lautz, J. and Müller, A. (1989) *Liebigs Ann. Chem., 913–928.*

Kim, Y. and Prestegard, J.H. (1990) Proteins, **8,** 377–385.

Ludvigsen, S., Andersen, K.V. and Poulsen, F.M. (1991) *J. Mol. Biol.*, **217,** 731–736.

Mierke, D.F. and Kessler, H. (1992) *Biopolymers,* **32,** 1277–1287.

Pardi, A., Billeter, M. and Wüthrich, K. (1984) *J. Mol. Biol.*, **180,** 741–751.

Pearlman, D.A. and Kollman, P.A. (1991) *J. Mol. Biol.*, **220,** 457–479.

Ryckaert, J.-P., Ciccotti, G. and Berendsen, H.J.C. (1977) *J. Comput. Phys.*, **23,** 327–341.

Shi Yun-yu, Wang Lu and van Gunsteren, W.F. (1988) *Mol. Sim.*, **1,** 369–388.

Torda, A.E., Scheek, R.M. and van Gunsteren, W.F. (1989) *Chem. Phys. Lett.*, **157,** 289–294.

Torda, A.E., Scheek, R.M. and van Gunsteren, W.F. (1990) *J. Mol. Biol.*, **214,** 223–235.

Van Gunsteren, W.F. and Berendsen, H.J.C. (1987) *Groningen Molecular Simulation (GROMOS) Library Manual,* Biomos, Groningen, The Netherlands.

Van Gunsteren, W.F. and Berendsen, H.J.C. (1988) *Mol. Sim.*, **1,** 173–185.

Wagner, G., Braun, W., Havel, T.F., Schaumann, T., Gõ, N. and Wüthrich, K. (1987) *J. Mol. Biol.*, **196,** 611–639.